

Original Article

Running Title: *Holothuria Leucospilota*-Derived Saponin and Gastric Cancer

Received: September 25, 2023; Accepted: April 16, 2024

Anticancer Activity of *Holothuria Leucospilota*-Derived Saponin on MNK45 Gastric Cancer Cell via Upregulation of *CDH1* Hub Gene

Khadijeh Sadegh^{*}, MSc, Amirhossein Ahmadi^{*♦}, PhD, Ahmad Shadi^{*}, PhD, Ahmad Ghasemi^{**},
PhD

^{*}*Department of Biological Science and Technology, Faculty of Nano- and Bio-Science and Technology, Persian Gulf University, Bushehr, Iran*

^{**}*Persian Gulf Research Institute, Persian Gulf University, Bushehr, Iran*

♦Corresponding Author

Amirhossein Ahmadi, PhD

Department of Biological Science and Technology,
Faculty of Nano- and Bio-Science and Technology,
Persian Gulf University, Bushehr, Iran

Email: ahahmadi@pgu.ac.ir

Abstract

Background: The treatment of gastric cancer (GC) is still quite challenging. Yet, marine invertebrates have been found to produce a wide range of anticancer bioactive compounds that show promise in fighting cancer. The present study aimed to evaluate whether saponin derived from *Holothuria leucospilata* (*H. Leucospilota*), a species of sea cucumber, possesses anti-cancer activity against GC cells.

Method: In this experimental study, the cytotoxic effect of *H. Leucospilota*-derived n-butanol fraction saponins (HLBS) sourced from the Persian Gulf on MNK45 GC cells was evaluated through tetrazolium salt and colony formation assays. The effect of HLBS on MNK45 cell migration, cell cycle, and apoptosis was assessed using a scratch assay, and flow cytometry, respectively. Hub genes of GC were identified through bioinformatics analysis. The effects of HLBS on the expression of the two top-ranked GC hub genes were measured using real-time polymerase chain reaction. Comparisons between groups were performed using the ANOVA test by GraphPad Prism software at the statistically significant *P*-value <0.05.

Results: HLBS with an IC₅₀ concentration of 75 µg/ml at 48 hours resulted in a significant decrease in cell viability, clonogenic ability (46.63% reduction, *P* < 0.01), and migration of MNK45 cells (74.5% reduction, *P* < 0.01). Moreover, HLBS led to an increase of approximately 21% and 13% in the S-phase and apoptotic cell populations, respectively. HLBS also upregulated the expression of *CDH1*, as a highly ranked hub gene associated with GC (*P* < 0.05).

Conclusion: The inhibitory effect of HLBS on MNK45 cells suggests HLBS as a candidate for further drug discovery programs in GC research, and paves the way to introduce new anti-cancer HLBS synthetic derivatives.

Keywords: Stomach neoplasms, Sea cucumber, Cadherins, Computational Biology

Introduction

Gastric cancer (GC) is the fifth most common malignancy and the fourth leading cause of cancer-related death worldwide.¹ While the incidence and mortality of GC have decreased in most parts of the world due to improved economic conditions and better food preservation practices in the last century, recent reports have shown an increase in the incidence rate of GC in younger adults (<50 years).¹

Dysregulation of gene expression plays a critical role in GC development.² Several high-throughput studies have been performed to profile dysregulated genes in GC, and hundreds of up- and down-regulated genes in GC have been reported.³ To achieve a short list of dysregulated genes with higher importance, several studies have used a system biology approach to introduce hub genes in GC that have many interactions with other genes in the network of dysregulated genes via computational and mathematical analysis.⁴ For example, Fibronectin-1 (*FNI*) and Cadherin-1 (*CDHI*) genes are two most reported hub genes in GC.^{2, 5, 6} *FNI* encodes fibronectin which is involved in cell motility, cell adhesion, and cell migration.⁷ *CDHI* is a tumor suppressor gene that encodes epithelial cadherin, and is involved in cell-cell adhesion, mobility, and proliferation of epithelial cells.⁸

Despite some advancements in GC prevention, the effectiveness of treatment for GC patients remains poor. Surgery is still the most powerful tool for treating GC, and when combined with chemotherapy based on 5-fluorouracil and cisplatin, it can improve patient survival by up to 15%.^{9, 10} However, the overall 5-year survival rate for patients with GC remains the lowest among all types of cancer.¹¹ Therefore, low survival rate of GC patients, side-effects of chemotherapeutic drugs, and drug resistance have led to a growing need for new therapeutic agents to treat GC.¹² The search

for natural bioactive compounds and their structural analogues with fewer adverse effects has always been a focus of drug discovery research. Several natural bioactive compounds including phenols, peptides, carbohydrates, fatty acids, alkaloids, terpenes, quinones, and saponins have proven to be anti-cancer substances. Interestingly, about 60% of current anti-cancer molecules were first discovered as natural bioactive compounds.¹³ Marine invertebrates are sources of diverse chemically bioactive lead compounds that can be the starting point of optimization in a drug discovery program. Therefore, marine organisms are under a wide range of screening to discover novel bioactive compounds such as anti-cancer agents.¹⁴ Cytarabine, trabectedin, eribulin mesylate, and monomethyl auristatin E are some examples of anti-cancer compounds derived primarily from marine organisms.¹⁵ Sea cucumbers are marine invertebrates belonging to the *Holothuroidea* class within the phylum Echinodermata, and comprise 1716 species.¹⁶ Some of these species, which have been used in traditional medicine in certain countries like China, have attracted the attention of researchers in recent decades due to their nutritive value and therapeutic properties.¹⁷ One of the most well-known bioactive compounds found in sea cucumbers are triterpene glycosides, also known as saponins.¹⁸ Saponins are secondary metabolites concentrated in the body walls and viscera of sea cucumbers. They consist of two parts: a triterpene backbone; and one to six monosaccharide units, with or without sulfate groups.¹⁹ Different types of saponins derived from sea cucumbers have shown anti-cancer properties against cancer cells by inducing apoptosis, arresting the cell cycle, reducing tumor growth, inhibiting metastasis and angiogenesis, and decreasing drug resistance. For example, Scabraside D, a saponin derived from *Holothuria scabra*, has shown a potent growth inhibitory effect

against GC cells.¹⁶ Additionally, violaceusides I, II, and III extracted from *Pseudocolochirus violaceus* have exhibited cytotoxic effects against a human GC cell line, MNK-45.²⁰ However, the effects of saponins derived from *Holothuria leucospilota* on GC cells have not been studied so far.

Holothuria leucospilota, commonly known as the black sea cucumber, is distributed in tropical regions around the world, from Northern Australia to the Indo Ocean and the Pacific Ocean. Furthermore, advances in breeding this species have made *Holothuria leucospilota* readily available. It is worth noting that high amounts of saponins are present in its cuvierian tubules and body walls.²¹ Therefore, the present study aims to evaluate the effects of *H. Leucospilota*-derived n-butanol fraction saponins (HLBS), obtained from the Persian Gulf, on a human gastric adenocarcinoma cell line. Specifically, the study investigates the effects of HLBS on GC cell cytotoxicity, migration, cell cycle, apoptosis, and colony formation. Moreover, the study examines the mRNA expression of some hub genes of GC under HLBS treatment.

Materials and Methods

Sampling

In this in vitro experimental study, *H. Leucospilota* were collected from the Persian Gulf coast in Bandar Abbas, Iran. After washing with distilled water, the body wall was separated and dried using freeze-drying equipment (CHRIST-Germany).

Extraction of crude saponin

The method described by Moghadam et al.²² was employed to extract crude saponin from the sea cucumber species *H. Leucospilota* with few changes. To extract the temperature-sensitive components, sea cucumber powder was soaked in 70% ethanol for 48 hours at 25°C. The resulting extract was filtered through Whatman paper (1 µm).

The remaining biomass was refluxed in 96% ethanol three times for 8 hours, and the supernatant was collected and filtered. The resulting extracts were evaporated using a rotary evaporator (Heidolph-Germany), and the residue was dissolved in water. The water phase was mixed with chloroform in a decanter and then separated. Subsequently, the water phase was mixed with n-butanol, and the n-butanol fraction was evaporated to obtain HLBS.

Fourier Transform Infrared (FTIR) Spectroscopy

FTIR analysis was conducted to compare the extracted HLBS with a standard saponin. To do so, HLBS powder was mixed with potassium bromide (KBr) and compressed to create a thin pellet for FTIR examination using an FTIR spectrometer (FTIR4600 Jasco-Japan) operating in absorbance mode, ranging from 4000 to 400 cm⁻¹.²³

Cell culture

The human gastric adenocarcinoma cell line MNK45 was obtained from the Stem Cell Technology Research Center (Tehran, Iran). The cells were cultured in high glucose Dulbecco's Modified Eagle Medium (DMEM) supplemented with 10% fetal bovine serum (FBS) and 1% penicillin/streptomycin in T25 flasks. The cells were maintained at 37°C in a humidified incubator with 5% CO₂ and 95% humidity. To detach MNK45 adherent cells from the Flask substrate for further tests, the culture media was removed and cells were washed with 1 ml phosphate-buffered saline (PBS). Next, PBS was removed and 1 ml Trypsin (0.025%)/EDTA (0.01%) solution was added and cells were incubated in incubator for 5 minutes. Finally, the effect of trypsin was blocked by adding 2 ml of DMEM contained 10% FBS. All culture vessels were obtained from SPL life Science-South Korea.

Cell viability assay

The cytotoxicity of HLBS was assessed using MTT (3-[4,5-dimethylthiazol-2-yl]-2,5-

diphenyl tetrazolium bromide) assay following the manufacturer's protocol (Bio-Idea, Iran). The optimal cell number for MTT assay was determined according to manufacturer's instruction. To perform a MTT assay a cell suspension of 4×10^3 cells/mL was seeded in 96-well plates and allowed to adhere for 24 hours. HLBS was dissolved in dimethyl sulfoxide (DMSO) (Bio-Idea, Iran) and then diluted with culture media. The final concentration of DMSO in the mixture was less than 0.1%. Cells were treated with different concentrations of the dissolved saponin (ranging from 50 to 400 $\mu\text{g/ml}$), and a concentration of 0.1% DMSO was used as a control. The plates were incubated at 37°C for 24 and 48 hours in a humidified atmosphere. MTT solution was then added and incubated at 37°C for 4 hours. The formazan crystals were then dissolved using 50 μL of lysis buffer (DMSO), and the absorbance was measured at 570 nm using a multi-well plate reader. The MTT assay was repeated three times with 6 replicates per treatment. To calculate the half maximal inhibitory concentration (IC_{50}) of HLBS six concentrations of HLBS (50, 100, 150, 200, 300 and 400 $\mu\text{g/mL}$) were used. By applying the linear regression equation, the IC_{50} value was determined, i.e., $Y = Mx + C$ in which $Y=50$ and $x=\text{IC}_{50}$.

Colony formation assay

The colony formation assay, considered a gold standard method, was utilized to measure the cytotoxic effect of HLBS as described in previous studies.²⁴ Briefly, a cell suspension of 2.7×10^4 cells/mL was seeded in a 6-well plate and incubated at 37 °C for 24 hours to allow the cells to adhere. Subsequently, the cells were treated with 75 $\mu\text{g/ml}$ HLBS or left untreated as control cells for 24 hours. In the next step, the cells from each well were counted, and 350 cells from each treated or untreated well were transferred to a new 6-well plate. The plate was then incubated at 37 °C for 14 days to

allow colony formation. Finally, the colonies were fixed with methanol and stained with 0.1% crystal violet, and colonies consisting of a minimum of 50 cells were counted. The percentage of plating efficiency (PE) and surviving fraction (SF) were calculated using the following equations:

$$PE = \frac{\text{number of colonies formed}}{\text{number of cells implanted}} \times 100,$$

$$SF = \frac{\text{number of colonies formed after treatment}}{\text{number of primary cultured cells} \times PE}$$

The colony formation assay was repeated three times with three replicates each time.

Wound healing assay

The wound healing assay is a significant and effective method used to measure cancer cell migration, where a scratch is created on a cell monolayer.²⁵ Briefly, a cell suspension of 8×10^5 cells/mL was seeded in a 6-well plate. After 24 hours, the culture medium in the wells was replaced with DMEM supplemented with 2% FBS, and the cells were then treated with 75 $\mu\text{g/ml}$ HLBS or left untreated as control cells. After 12 hours, the wells were scratched using a micropipette tip, and each well was washed with PBS. The culture medium containing 2% FBS was added back to the wells, and images were captured at 0 and 24 hours to observe cell migration. The images were analyzed by Image J software (Version 1.53) to quantify the rate of migration and wound closure. The wound healing assay was repeated three times with three replicates each time.

Cell cycle assay

A total of 2×10^5 cells were seeded in 6-well plates until reaching 70% confluence. Subsequently, the cells were treated with 75 $\mu\text{g/ml}$ HLBS or left untreated as control cells and incubated at 37 °C for 48 hours. Next, the cells were washed with cold saline phosphate buffer and fixed with 70% ethanol. 0.5 ml Propidium iodide (PI) supplemented with RNase A (FxCycle™, Thermo Fisher) was added to the fixed cells at the final concentration of 10 and 0.5 $\mu\text{g/ml}$,

respectively; and incubated at 37 °C for 30 minutes in the dark. Finally, flow cytometry (BD Biosciences, USA) was employed to measure the percentage of cells in different phases of the cell cycle. The cell cycle assay was repeated three times with three replicates each time.

Apoptotic and necrotic assay

PI and fluorescein isothiocyanate (FITC)-conjugated Annexin V (Annexin V-FITC) staining is a standard method for measuring apoptosis and necrosis using flow cytometry.²⁶ Briefly, 2×10^5 cells were cultured in a 6-well plate until reaching 70% confluence. Subsequently, the cells were treated with 75 µg/ml HLBS or left untreated as control cells and incubated at 37 °C for 48 hours. Then, the cells were washed twice with PBS and trypsinized, and 4×10^5 cells resuspended in 200 µl Annexin V binding buffer following the manufacturer's protocol of the apoptosis detection kit (Biolegend, USA). Next, 100 µl cell suspension was transferred to a new microtube and 5 µl of FITC Annexin V and 10 µL of PI Solution was added and incubated for 15 min at room temperature in the dark. Finally, 400 µl Binding Buffer was added to each test microtube and the stained cells were analyzed using flow cytometry (BD Biosciences, USA) to determine the percentage of apoptotic and necrotic cells. The Annexin V/PI assay was repeated three times with three replicates each time.

Extraction the hub genes of GC

In the present study, a dataset of high-density oligonucleotide microarray was utilized to identify hub genes associated with GC. The dataset used was GSE54129, which was obtained from the GEO database (<http://www.ncbi.nlm.nih.gov/geo/>). The dataset was generated using the GPL570 platform [HG-U133_Plus_2], which corresponds to the Affymetrix Human Genome U133 Plus 2.0 Array. It consisted of

111 human GC tissues and 21 gastric healthy tissues.

To analyze the dataset, R software (<https://rstudio.com/products/rstudio/download/>) was employed, along with the Biobase, GEOquery, and limma packages. These packages were utilized to identify the differentially expressed genes (DEGs) between the tumor and normal samples of GSE54129. DEGs with $|\log_2FC| > 1.5$ and a P -value < 0.05 were considered statistically significant and used for further analysis.

To explore the protein-protein interaction (PPI) networks of DEGs, the STRING database was utilized. The interaction networks were constructed, and to identify the hub genes associated with GC, CytoHubba, a Cytoscape plugin, was employed. This plugin enabled the exploration of the PPI network and the identification of hub genes in GC.

Real-time polymerase chain reaction (PCR)

To study the expression of *FNI* and *CDHI* under HLBS treatment, a total of 2×10^5 cells were seeded in 6-well plates until reaching 70% confluence. Subsequently, the cells were treated with 75 µg/ml HLBS or left untreated as control cells and incubated at 37 °C for 48 hours. Total RNA was isolated using 1ml of RNX plus solution (Sinaclon, Iran) following the manufacturer's instructions. To ensure the quality and quantity of the extracted RNA, agarose gel electrophoresis and a spectrophotometer were used. 1 µg of RNA was treated with 1 unit of DNase I (1U/µl) (Thermoscientific, USA) and then reverse transcribed using the M-MuLV Reverse Transcriptase of the cDNA Synthesis Kit (SinaClon, Iran) according to the manufacturer's protocol.

For studying alterations in gene expression, real-time PCR was performed using the Rotor Gene Q system (Qiagen, USA), 10 µl RealQ Plus 2x Master Mix Green Without ROX (Ampliqon-Denmark), 0.7 µl of each primer working solution (10 pM), and 10 ng

of cDNA template in a final reaction volume of 20 μ l. The primer sequences (SinaClon, Iran) were presented in table 1. The thermal reaction condition was as follows: initial denaturation at 95 °C for 15 min, followed by 35 cycles of denaturation at 95 °C for 15 sec, annealing at 60 °C for 30 sec, and extension at 72 °C for 20 sec. Specificity of PCR products were verified using poly acrylamide gel electrophoresis and dissociation melt curve analysis. The expression of each gene was normalized to the β -Actin (ACTB) mRNA as a housekeeping and control gene and Δ Cts were calculated by the difference between Ct of the target genes and Ct of ACTB. Relative expression was calculated by $2^{-\Delta\Delta C_t}$ formula. A no reverse transcribed RNA sample was used to control DNA contamination and a sample that contained no cDNA template (Negative control) were used to check PCR false amplification for each gene amplification in each run of real time PCR.

Statistical analysis

Statistical analyses were conducted using GraphPad Prism software (version 9). All data were presented as means \pm standard deviation (SD) of three independent experiments. Comparisons between groups were performed using analysis of variance (ANOVA) followed by post-hoc tests or independent t-tests, as appropriate. A *P*-value of less than 0.05 was considered statistically significant.

Results

FTIR confirmed the triterpenoid content of HLBS

To confirm the presence of terpenoids in HLBS, the functional groups of HLBS were analyzed using FTIR. Figure 1 displays selected peaks from the FTIR spectrum of the n-butanol fraction of *H. leucospilota*, which were compared with the FTIR spectrum of standard saponins previously reported.²⁷ The presence of hydroxyl groups (-OH) was

indicated by a long, sharp peak observed at 3353.6 cm^{-1} . The peak at 2919.7 cm^{-1} and 2852.2 cm^{-1} displayed two or three bands, representing the stretching vibrations of alkyl groups (C-H). Furthermore, an evident absorption peak at 1052.94 cm^{-1} indicated the presence of oligosaccharide linkages to saponins (C-O-C). The stretching of the carbonyl group was apparent at 1641 cm^{-1} (Table 2). These characteristic peaks confirmed the presence of terpenoids in the extracted fraction.

Cell viability assay demonstrated the cytotoxicity of HLBS on MNK45 cells

The cytotoxic effect of HLBS on MNK45 cells was evaluated using the MTT assay (Figure 2A). The results indicate that 0.1% DMSO, which served as the solvent for HLBS, did not significantly affect cell viability as compared to the control cells.

In contrast, different concentrations of HLBS exhibited a cytotoxic effect on MNK45 cells in a time and dose-dependent manner. For instance, at a concentration of 75 $\mu\text{g}/\text{mL}$, HLBS inhibited the growth of MNK45 cells by 22% after 24 hours and 50% after 48 hours (Figure 2A). This demonstrates that higher concentrations of HLBS resulted in a stronger inhibitory effect on cell growth over time. Moreover, the half-maximal inhibitory concentration (IC_{50}) of HLBS was determined to be 400 and 75 $\mu\text{g}/\text{mL}$ after 24 and 48 hours of treatment, respectively.

Colony formation assay

The colonization test was employed as a standard method to assess the long-term effects of HLBS on MNK45 cells at a concentration of 75 $\mu\text{g}/\text{mL}$. Figure 2B illustrates that HLBS treatment at this concentration led to a reduction in colonization of MNK45 cells.

To quantify the extent of this effect, the number of colonies in both control and treated cells was counted. The data revealed that after two weeks from the initiation of the test, the survival rate of the treated cells

decreased by 55% as compared with the control cells (Figure 2C). This suggests that HLBS at a concentration of 75 µg/ml significantly impeded the ability of MNK45 cells to form colonies and survive over the long term.

The information presented in figure 3 highlights the potential long-term inhibitory impact of HLBS on MNK45 cells, as observed through the colonization test.

HLBS inhibited the migration ability of MNK45 cells

The scratch assay performed to assess the effect of HLBS at a concentration of 75 µg/ml on the migration intensity of MNK45 cells. In figure 3A, it is evident that HLBS treatment led to a decrease in the migration capability of MNK45 cells. This suggests that HLBS impaired the ability of the cells to migrate and close the wound created in the scratch assay. To quantify the extent of this effect, the wound area was measured and analyzed using Image J software. The results, as shown in figure 3B, indicate that the wound closure for cells treated with HLBS was approximately 45% lower than the wound closure for untreated cells during the 24 hours after treatment. This indicates a significant reduction in the migration of MNK45 cells in response to HLBS treatment. The findings from the scratch assay demonstrate that HLBS at a concentration of 75 µg/ml effectively inhibits the migration capability of MNK45 cells.

HLBS arrested MNK45 cells at S phase

The effect of HLBS (75 µg/ml) on the cell cycle was evaluated by flow cytometry at 48 hours after treatment (Figure 4A). The results indicate that HLBS treatment decreased the population of cells in the G1 phase of the cell cycle. The percentage of cells in the G1 phase among the control cells was 52.47%, whereas in HLBS-treated cells, it decreased to 29.63%. Conversely, the data also shows that HLBS treatment increased the population of cells in the S phase of the cell cycle. Among

the control cells, the percentage of cells in the S phase was 34.03%, but after HLBS treatment, it increased to 55.58% (Figure 4B). The increase in the S phase population indicates that HLBS may cause cells to accumulate in the S phase, suggesting a possible S phase cell cycle arrest.

HLBS induced cell apoptosis

To evaluate the effect of HLBS (75 µg/ml) on apoptosis of MNK45 cells, Annexin-PI staining was performed and data analysis were conducted by flow cytometry at 48 hours after treatment (Figure 4C). According to the data, HLBS treatment led to a significant increase in the percentage of apoptotic cells compared with untreated cells. As shown in figure 4D, about 13% of MNK45 cells underwent apoptosis after treatment with HLBS.

Importantly, the data also indicates that HLBS-induced apoptosis was the dominant form of programmed cell death in MNK45 cells. The percentage of necrotic cells among the treated cells was only about 5%, which is considerably lower than the percentage of apoptotic cells.

FNI and CDH1 were found as GC hub genes with the highest score

Bioinformatic analysis conducted using R software identified 1327 differentially expressed genes between normal and tumor samples in GC. To further investigate the potential functional interactions among these differentially expressed genes, a PPI network was constructed using the STRING database (Data not shown) and the 10 hub genes were extracted from the PPI network. Table 3 lists 10 identified hub genes, ranked based on their node degree, which represents the number of connections each gene has in the protein-protein interaction network. Among the identified hub genes, *FNI* was found to be upregulated in GC as compared with normal samples, while *CDH1* was downregulated. Both of these genes displayed the highest scores in their

respective directions of regulation, suggesting that they might be crucial players in the pathogenesis of GC.

To assess the impact of HLBS on the differential expression of hub genes, *FNI* and *CDH1* were selected for further investigation. *FNI*, as an upregulated hub gene, and *CDH1*, as a downregulated hub gene, represent potential targets of saponin treatment in the context of GC.

Real-time PCR confirmed the up-regulation of CDH1 under HLBS treatment

To examine alterations in the expression of *CDH1* and *FNI* genes in cells treated with HLBS, real-time PCR analysis was performed at 48 hours after treatment. As shown in figure 4E, HLBS increased the expression of *CDH1* genes. While the expression of *FNI* in treated cells was unchanged, a 3-fold increase in *CDH1* expression was observed compared with control cells.

Discussion

In this study, we showed that HLBS with an IC_{50} concentration of 75 $\mu\text{g/ml}$ resulted in a significant decrease in cell viability, clonogenic ability (46.63% reduction, $P < 0.01$), and cell migration of MNK45 cells (74.5% reduction, $P < 0.01$). Moreover, treatment with 75 $\mu\text{g/ml}$ of HLBS for 48 hours led to an increase of approximately 21% and 13% in the S-phase and apoptotic cell populations, respectively. HLBS also upregulated the expression of *CDH1*, as a highly ranked hub gene associated with GC ($P < 0.05$) (Figure 5).

In this study, we employed a liquid-liquid extraction method to obtain HLBS. The organic n-butanol fraction offers advantages over an aqueous solution, including enhanced purity, greater bioactivity, and a more diverse saponin profile.²⁸ However, it is worth noting that water-soluble saponins may have been lost during the n-butanol fraction extraction in our study.

Confirmation of the presence of saponin in the n-butanol fraction was achieved through FTIR analysis. Our FTIR data aligns with previous studies that reported characteristic peaks in the FTIR spectrum of sea cucumbers, such as hydroxyl groups (-OH) at 3353.6 cm^{-1} , alkyl groups (C-H) at 2919.7 and 2852.2 cm^{-1} , a γ -lactone group at 1737.55 cm^{-1} , and oligosaccharide linkage absorption to saponins (C-O-C) at 1052.94 cm^{-1} .²⁹ Although we did not employ NMR and chromatography methods to detect individual components of the n-butanol-extracted saponin, previous research on organic extracts of saponin from Persian Gulf *H. leucospilota* reported the presence of main components like echinoside A, holothurine A, and 24-dehydroechinoside A,³⁰ which might be present in our extract as well.

We observed the cytotoxicity of HLBS with an IC_{50} of 75 $\mu\text{g/ml}$ on MNK45 cell line after 48 hours of treatment. While there are no published data on the effect of HLBS on gastric cancer cells, several studies have demonstrated the cytotoxic effects of *H. leucospilota*-derived saponins on other cancer cell lines. In another study, after extracting butanol, aqueous, hexane, and dichloromethane fractions of *H. leucospilota*, Shushizadeh, et al. reported that n-butanol extract inhibited the proliferation of cervical cancer cell line (HeLa) at a lower concentration than the other fractions with IC_{50} of 129 $\mu\text{g/ml}$.³⁰ Notably, gastric MNK45 cells appeared more sensitive to extracted HLBS as compared with cervical cancer HeLa cells, suggesting potential selectivity for cancer cells. In contrast to our study, Shushizadeh et al. also evaluated the cytotoxicity of extracted saponin on non-cancer Huvec cells and found that *H. leucospilota*-derived saponins were more toxic for cancer cells.³⁰ Also, Khaledi et al. demonstrated that *H. leucospilota* methanolic extract has cytotoxicity on the breast cancer cell line (SK-BR-3) with IC_{50} of 50 $\mu\text{g/ml}$ at

48 hours but its cytotoxicity was about 2.5 fold lower on normal fibroblast cell line (MCR5).³¹

Furthermore, our colony formation assay confirmed the cytotoxic effects of HLBS on MNK45 cells. This aligns with previous studies that have shown the inhibitory effects of sea cucumber-derived saponins on cancer cell colony formation in various cancer types. For example, Methanolic extract from the body wall of *H. scabra* decreased the colony-forming in human prostate cancer cell line (PC3).³² Six new triterpene oligoglycosides of the sea cucumber *Cladolabes schmeltzii* inhibited the colony formation and growth of human colorectal adenocarcinoma HT-29 cells.³³ Stichoposide C (STC) a triterpene glycoside isolated from sea cucumber *Thelenota ananas* reduced the colony formation of human ovarian cancer (A2780 and SKOV3) cell lines.³⁴

Interestingly, we observed S-phase cell cycle arrest in MNK45 cells after treatment HLBS. Inducing cell cycle arrest at the S-phase has significant implications in cancer treatment, as it can actively target dividing cancer cells and increase their sensitivity to DNA-damaging agents. However, our findings contrast with some studies that reported different effects of saponins on the cell cycle, possibly due to variations in saponin components used in those studies. For example, *H. leucospilota*-derived saponin was shown to increase sub-G1 peak in MCF7 breast cancer cells and B16F10 melanoma cells.^{29, 35} Pranweerapaiboon et al. reported that *H. nobilis Selenka*-derived echinoside A induced G0/G1 cell cycle arrest in prostate cancer PC3 cells.³² In another study, ethanolic extracts from black-spotted sea cucumber *Pearsonothuria graeffei* (Pg) was shown to induce the G0/G1 phase arrest in liver cancer HepG2 cells.³⁶

Apoptosis (4% early and 9% late apoptosis) was also induced in MNK45 cells following S-phase cell cycle arrest upon treatment with

HLBS. It is important to note that distinguishing between necrotic and late apoptotic cell populations can be quite challenging when using a flow cytometer, as their characteristics can often overlap. Additional assays such as measuring cleaved caspase is necessary to confirm flow cytometer data. However, induction of apoptosis aligns with previous reports that showed *H. leucospilota* saponins inducing apoptosis in cancer cell lines.^{29, 35} This could be associated with changes in the expression of Bax, caspase-3, caspase-7, and Bcl-2, as reported in SK-BR-3 breast cancer cells treated with *H. leucospilota*-derived saponins.³¹

Furthermore, our study revealed that HLBS inhibited the migratory potential of MNK45 cells, indicating their potential as agents to suppress metastasis. This finding is consistent with previous reports of sea cucumber saponins inhibiting cell migration in other cancer cell lines.^{32, 37}

To investigate whether the anti-cancer effects of HLBS were associated with the modulation of gastric cancer hub genes, we predicted 10 hub genes associated with gastric cancer in this study. Our findings were consistent with previous studies that identified key genes, such as *FNI*, *CDHI*, *MMP2*, *MMP9*, and *CTNNB1*, associated with gastric cancer.^{2, 38}

Among the hub genes, we evaluated the expression of *FNI* and *CDHI* in HLBS-treated MNK45 cells. *FNI* is a glycoprotein molecule³⁹ expressed by different cell types, and is involved in cell adhesion, proliferation and migration, including metastasis.⁴⁰ *FNI* was elevated in different malignancies such as hepatocellular carcinoma, renal, head/neck, and gastrointestinal cancer.⁴¹ Decreasing the expression of *FNI* inhibits gastric cancer cell migration, enhancing apoptosis and invasion in vitro.⁴² In this study, while the expression of *FNI* was unaffected, *CDHI* was significantly

upregulated by the HLBS treatment. Instead, the mRNA expression of *CDHI* was increased in MNK45 cells under treatment by HLBS. *CDHI* encodes Cadherin-1, as a calcium-dependent cell-cell adhesion glycoprotein has an important function in maintaining cell adhesion and adherent junction in healthy tissues. *CDHI* plays a crucial role in maintaining cell adhesion and tissue organization, and its dysregulation is linked to invasion and metastasis in various cancers, including gastric cancer.⁴³ Studies show that mutations such as inactivating mutations or promoter methylation in *CDHI* increase the risk of gastric cancer.⁴⁴ The mechanism by which HLBS upregulate *CDHI* remains unclear, but it is possible that they reverse promoter hypermethylation, as previously reported for ginseng saponins in colorectal cancer cells.⁴⁵

To the best of our knowledge, this is the first study to evaluate the anti-cancer effects of saponin extracted from *H. leucospilota* on gastric adenocarcinoma cells; however, this study also has two main limitations. First, although we identified the extracted HLBS using FTIR, we did not employ GC/MS to detect all HLBS components. Second, we only evaluated the effects of the n-butanol fraction, and the potential effects of other organic or aqueous fractions were not explored.

Conclusion

The present study sheds light on the anti-cancer effects of HLBS on gastric adenocarcinoma cells. Our results indicate that sea cucumber saponins have the potential to be considered as promising sources of new anticancer compounds, especially the possibility of controlled farming for sustainable extraction. However, our understanding of the therapeutic potential of these natural bioactive metabolites for GC treatment is further enhanced once we address the limitations of the study, such as

identifying all HLBS components and exploring other saponin fractions. Synthesis of different derivatives of HLBS and studying their anti-cancer effects on GC in vitro and in vivo alone or in combination with conventional anti-cancer drugs is suggested for future investigations.

Acknowledgments

The authors are grateful to the research management of the Persian Gulf Research Institute for providing this research opportunity. The authors received no financial support for this study.

Data Availability

The data that support the findings of this study are openly available in the National Centre for Biotechnology Information Gene Expression Omnibus (NCBI-GEO) under the Accession number GSE54129.

Conflict of Interest

None declared.

References

1. Morgan E, Arnold M, Camargo MC, Gini A, Kunzmann AT, Matsuda T, et al. The current and future incidence and mortality of gastric cancer in 185 countries, 2020-40: A population-based modelling study. *EClinicalMedicine*. 2022;47:101404. doi: 10.1016/j.eclinm.2022.101404.
2. Sadegh K, Ahmadi A. Hub genes and pathways in gastric cancer: A comparison between studies that used normal tissues adjacent to the tumour and studies that used healthy tissues as calibrator. *IET Syst Biol*. 2023;17(3):131-41. doi: 10.1049/syb2.12065.
3. Lin X, Zhao Y, Song WM, Zhang B. Molecular classification and prediction in gastric cancer. *Comput Struct Biotechnol J*. 2015;13:448-58. doi: 10.1016/j.csbj.2015.08.001.

4. Mottaghi-Dastjerdi N, Ghorbani A, Montazeri H, Guzzi PH. A systems biology approach to pathogenesis of gastric cancer: gene network modeling and pathway analysis. *BMC Gastroenterol.* 2023;23(1):248. doi: 10.1186/s12876-023-02891-4.
5. Han C, Jin L, Ma X, Hao Q, Lin H, Zhang Z. Identification of the hub genes RUNX2 and FN1 in gastric cancer. *Open Med (Wars).* 2020;15(1):403-12. doi: 10.1515/med-2020-0405.
6. Lu XQ, Zhang JQ, Zhang SX, Qiao J, Qiu MT, Liu XR, et al. Identification of novel hub genes associated with gastric cancer using integrated bioinformatics analysis. *BMC Cancer.* 2021;21(1):697. doi: 10.1186/s12885-021-08358-7.
7. Hsiao CT, Cheng HW, Huang CM, Li HR, Ou MH, Huang JR, et al. Fibronectin in cell adhesion and migration via N-glycosylation. *Oncotarget.* 2017;8(41):70653-68. doi: 10.18632/oncotarget.19969.
8. Shenoy S. CDH1 (E-cadherin) mutation and gastric cancer: genetics, molecular mechanisms and guidelines for management. *Cancer Manag Research.* 2019;11:10477. doi: 10.2147/CMAR.S208818.
9. Orditura M, Galizia G, Sforza V, Gambardella V, Fabozzi A, Laterza MM, et al. Treatment of gastric cancer. *World J Gastroenterol.* 2014;20(7):1635-49. doi: 10.3748/wjg.v20.i7.1635.
10. Sitarz R, Skierucha M, Mielko J, Offerhaus GJA, Maciejewski R, Polkowski WP. Gastric cancer: epidemiology, prevention, classification, and treatment. *Cancer Manag Res.* 2018;10:239. doi: 10.2147/CMAR.S149619.
11. Thrift AP, El-Serag HB. Burden of gastric cancer. *Clin Gastroenterol Hepatol.* 2020;18(3):534-42. doi: <https://doi.org/10.1016/j.cgh.2019.07.045>.
12. Liu YQ, Wang XL, He DH, Cheng YX. Protection against chemotherapy-and radiotherapy-induced side effects: A review based on the mechanisms and therapeutic opportunities of phytochemicals. *Phytomedicine.* 2021;80:153402. doi: 10.1016/j.phymed.2020.153402.
13. Law JW, Law LN, Letchumanan V, Tan LT, Wong SH, Chan KG, et al. Anticancer drug discovery from microbial sources: the unique mangrove streptomycetes. *Molecules.* 2020;25(22):5365. doi: 10.3390/molecules25225365.
14. Patra S, Praharaj PP, Panigrahi DP, Panda B, Bhol CS, Mahapatra KK, et al. Bioactive compounds from marine invertebrates as potent anticancer drugs: the possible pharmacophores modulating cell death pathways. *Mol Biol Rep.* 2020;47(9):7209-28. doi: 10.1007/s11033-020-05709-8.
15. Adrian TE, Collin P. The anti-cancer effects of frondoside A. *Mar drugs.* 2018;16(2):64. doi: 10.3390/md16020064.
16. Pangestuti R, Arifin Z. Medicinal and health benefit effects of functional sea cucumbers. *J Tradit Complement Med.* 2018;8(3):341-51. doi: 10.1016/j.jtcme.2017.06.007.
17. Yu S, Ye X, Huang H, Peng R, Su Z, Lian XY, et al. Bioactive sulfated saponins from sea cucumber *Holothuria moebii*. *Planta Med.* 2015;81(2):152-9. doi: 10.1055/s-0034-1383404.
18. Luparello C, Ragona D, Asaro DML, Lazzara V, Affranchi F, Celi M, et al. Cytotoxic potential of the coelomic fluid extracted from the sea cucumber *Holothuria tubulosa* against triple-negative MDA-MB231 breast cancer cells. *Biology.* 2019;8(4):76. doi: 10.3390/biology8040076.
19. Podolak I, Grabowska K, Sobolewska D, Wróbel-Biedrawa D, Makowska-Wąs J, Galanty A. Saponins as cytotoxic agents: an update (2010–2021). Part II—Triterpene saponins. *Phytochem Rev.* 2023;22:113-67. <https://doi.org/10.1007/s11101-022-09830-3>.

20. Khotimchenko Y. Pharmacological potential of sea cucumbers. *Int J Mol Sci.* 2018;19(5):1342. doi: 10.3390/ijms19051342.
21. Malaiwong N, Chalorak P, Jattujan P, Manohong P, Niamnont N, Suphamungmee W, et al. Anti-Parkinson activity of bioactive substances extracted from *Holothuria leucospilota*. *Biomed Pharmacother.* 2019;109:1967-77. doi: 10.1016/j.biopha.2018.11.063.
22. Moghadam FD, Baharara J, Balanezhad SZ, Jalali M, Amini E. Effect of *Holothuria leucospilota* extracted saponin on maturation of mice oocyte and granulosa cells. *Res Pharm Sci.* 2016;11(2):130-7.
23. Soltani M, Parivar K, Baharara J, Kerachian MA, Asili J. Hemolytic and cytotoxic properties of saponin purified from *Holothuria leucospilota* sea cucumber. *Rep Biochem Mol Biol.* 2014;3(1):43-50.
24. Siragusa M, Dall'Olio S, Fredericia PM, Jensen M, Groesser T. Cell colony counter called CoCoNut. *PloS one.* 2018;13:e0205823. doi: 10.1371/journal.pone.0205823.
25. Justus CR, Leffler N, Ruiz-Echevarria M, Yang LV. In vitro cell migration and invasion assays. *J Vis Exp.* 2014;(88):51046. doi: 10.3791/51046.
26. Brauchle E, Thude S, Brucker SY, Schenke-Layland K. Cell death stages in single apoptotic and necrotic cells monitored by Raman microspectroscopy. *Sci Rep.* 2014;4:1-9. doi: 10.1038/srep04698.
27. Kartikaningsih H, A'yunin Q, Soeprijanto A, Arifin NB, editors. Black sea cucumber (*Holothuria atra*) ethanol extract as *Edwardsiella tarda* antibacterial. *AIP Conf. Proc.* 2019; 060010-1–060010-9. doi:10.1063/1.5061919.
28. Plaskova A, Mlcek J. New insights of the application of water or ethanol-water plant extract rich in active compounds in food. *Front Nutr.* 2023;10:1118761. doi: 10.3389/fnut.2023.1118761.
29. Soltani M, Parivar K, Baharara J, Kerachian MA, Asili J. Putative mechanism for apoptosis-inducing properties of crude saponin isolated from sea cucumber (*Holothuria leucospilota*) as an antioxidant compound. *Iran J Basic Med Sci.* 2015;18(2):180-7.
30. Shushizadeh MR. Phytochemical analysis of *Holothuria leucospilota*, a sea cucumber from Persian Gulf. *Res Pharm Sci.* 2019;14(5):432-40. doi: 10.4103/1735-5362.268204.
31. Khaledi M, Moradipoodeh B, Moradi R, Baghbadorani MA, Mahdavinia M. Antiproliferative and proapoptotic activities of Sea Cucumber *H. Leucospilota* extract on breast carcinoma cell line (SK-BR-3). *Mol Biol Rep.* 2022;49(2):1191-200. doi: 10.1007/s11033-021-06947-0.
32. Pranweerapaiboon K, Noonong K, Apisawetakan S, Sobhon P, Chaithirayanon K. Methanolic extract from sea cucumber, *holothuria scabra*, induces apoptosis and suppresses metastasis of PC3 prostate cancer cells modulated by MAPK signaling pathway. *J Microbiol Biotechnol.* 2021;31(6):775-83. doi: 10.4014/jmb.2103.03034.
33. Silchenko AS, Kalinovskiy AI, Avilov SA, Andryjaschenko PV, Dmitrenok PS, Yurchenko EA, et al. Cladolosides O, P, P1-P3 and R, triterpene glycosides with two novel types of carbohydrate chains from the sea cucumber *Cladolabes schmeltzii*. Inhibition of cancer cells colony formation and its synergy with radioactive irradiation. *Carbohydr Res.* 2018;468:73-9. doi: 10.1016/j.carres.2018.08.004.
34. Liu F, Tang L, Tao M, Cui C, He D, Li L, et al. Stichoposide C exerts anticancer effects on ovarian cancer by inducing autophagy via inhibiting AKT/mTOR pathway. *Oncotargets Ther.* 2022;15:87. doi: 10.2147/OTT.S340556.

35. Baharara J, Amini E, Nikdel N, Salek-Abdollahi F. The cytotoxicity of dacarbazine potentiated by sea cucumber saponin in resistant B16F10 melanoma cells through apoptosis induction. *Avicenna J Med Biotechnol.* 2016;8(3):112.
36. Cui H, Bashar MA, Rady I, El-Naggar HA, El-Maoula A, Lamiaa M, et al. Antiproliferative activity, proapoptotic effect, and cell cycle arrest in human cancer cells of some marine natural product extract. *Oxid Med Cell Longev.* 2020;2020:7948705 doi: 10.1155/2020/7948705.
37. Ru R, Guo Y, Mao J, Yu Z, Huang W, Cao X, et al. Cancer cell inhibiting sea cucumber (holothuria leucospilota) protein as a novel anti-cancer drug. *Nutrients.* 2022;14(4):786. doi: 10.3390/nu14040786.
38. Sun C, Yuan Q, Wu D, Meng X, Wang B. Identification of core genes and outcome in gastric cancer using bioinformatics analysis. *Oncotarget.* 2017;8(41):70271. doi: 10.18632/oncotarget.20082.
39. Zhou Y, Cao G, Cai H, Huang H, Zhu X. The effect and clinical significance of FN1 expression on biological functions of gastric cancer cells. *Cell Mol Biol (Noisy-le-grand).* 2020;66(5):191-8.
40. Cai X, Liu C, Zhang TN, Zhu YW, Dong X, Xue P. Down-regulation of FN1 inhibits colorectal carcinogenesis by suppressing proliferation, migration, and invasion. *J cell Biochem.* 2018;119(6):4717-28.
41. Zhou Y, Shu C, Huang Y. Fibronectin promotes cervical cancer tumorigenesis through activating FAK signaling pathway. *J Cell Biochem.* 2019;120(7):10988-97. doi: 10.1002/jcb.28282.
42. Sun Y, Zhao C, Ye Y, Wang Z, He Y, Li Y, et al. High expression of fibronectin 1 indicates poor prognosis in gastric cancer. *Oncol Lett.* 2020;19(1):93-102. doi: 10.3892/ol.2019.11088.
43. Melo S, Figueiredo J, Fernandes MS, Gonçalves M, Morais-de-Sá E, Sanches JM, et al. Predicting the functional impact of CDH1 missense mutations in hereditary diffuse gastric cancer. *Int J Mol Sci.* 2017;18(2):2687. doi: 10.3390/ijms18122687.
44. Kheirollahi M, Saneipour M, Tabatabaiefar MA, Zeinalian M, Minakari M, Moridnia A. New variants in the CDH1 gene in Iranian families with hereditary diffuse gastric cancer. *Middle East J Cancer.* 2020;11(4):493-501. doi: 10.30476/mejc.2020.81478.1016.
45. Kang KA, Kim HS, Kim DH, Hyun JW. The role of a ginseng saponin metabolite as a DNA methyltransferase inhibitor in colorectal cancer cells. *Int J Oncol.* 2013;43(1):228-36. doi: 10.3892/ijo.2013.1931.

Table 1. The Primer sequences used in real-time PCR

Gene	Primer sequences	Product length (base pairs)
<i>FNI</i>	Forward: 5'-TGGGCAACTCTGTCAACGAAGG-3' Reverse: 5'-GACCACTTCCAAAGCCTAAGCAC-3'	184
<i>CDHI</i>	Forward: 5'-GCCTCCTGAAAAGAGAGTGGGAAG-3' Reverse: 5'-TGGCAGTGTCTCTCCAAATCCG-3'	131
<i>ACTB</i>	Forward: 5'-AGCCTTCCTCCTGGGCATGG-3'; Reverse: 5'-AGCACTGTGTTGGCGTACAGGTC-3'	106

FNI: Fibronectin-1, *CDHI*: Cadherin 1, *ACTB*: Beta-actin; PCR: Polymerase chain reaction

Table 2. Functional groups of n-butanol fraction of *H.leucospilota* extract

Number	Absorption (nm)	Reference	Functional group
1	3353.6	3300-3600	OH
2	2919.7	2960-2850	C-H
3	2852.2		
4	1737.55	1730-1680	C=O
5	1641.13		
10	1052.94	1150-1040	C-O-C
11	973.876	970-960	RHC=CHR
12	833.098	840-790	
13	719.318	720-680	Aromatic ring
14	620.966		

Table 3. The ten hub genes of GC that ordered according to their scores.

Name	Rank	score	Expression
FN1	1,9606	188.0	Up regulated
IL6	2,9606	180.0	Up regulated
CDH1	3,9606	119.0	Down regulated
MMP9	3,9606	119.0	Up regulated
CXCL8	5,9606	116.0	Up regulated
CTNNB1	6,9606	110.0	Down regulated
CD44	7,9606	109.0	Up regulated
CDC42	8,9606	98.0	Up regulated
MMP2	9,9606	96.0	Up regulated
IGF1	9,9606	96.0	Up regulated

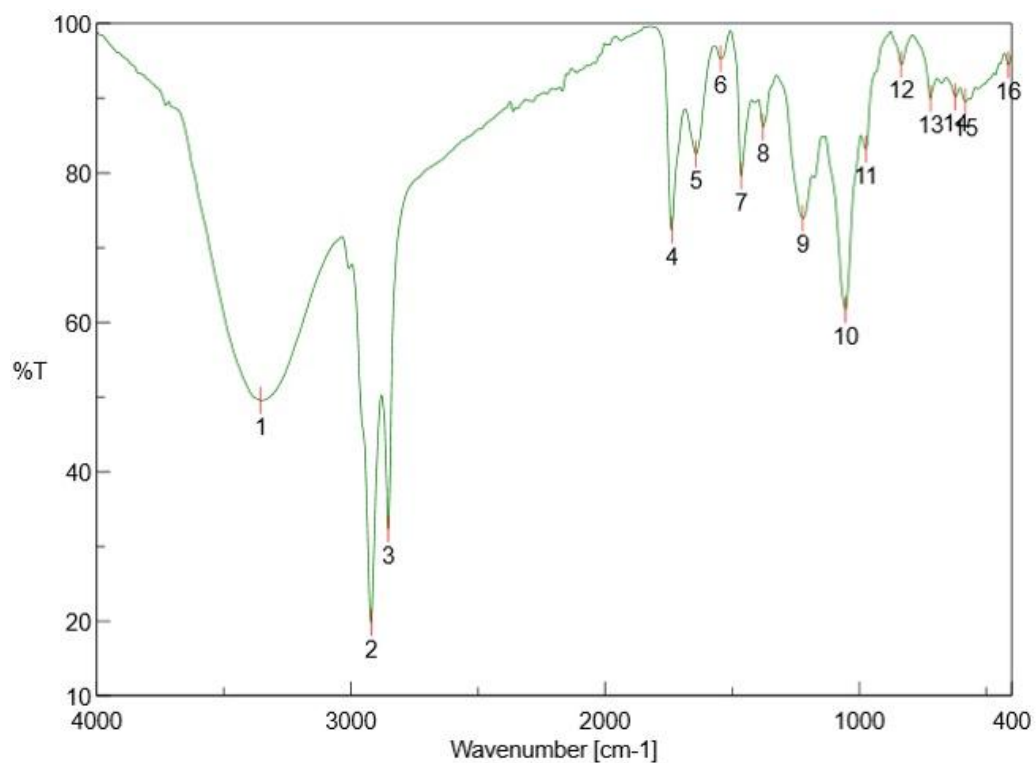


Figure 1. FTIR spectrum of *H. Leucospilota*-derived n-butanol fraction saponins. The presence of hydroxyl groups (-OH) was indicated by a long, sharp peak observed at 3353.6 cm^{-1} . The peak at 2919.7 cm^{-1} and 2852.2 cm^{-1} displayed two or three bands, representing the stretching vibrations of alkyl groups (C-H). Furthermore, an evident absorption peak at 1052.94 cm^{-1} indicated the presence of oligosaccharide linkages to sapogenins (C-O-C). The stretching of the carbonyl group was apparent at 1641 cm^{-1} .

T: Transmittance

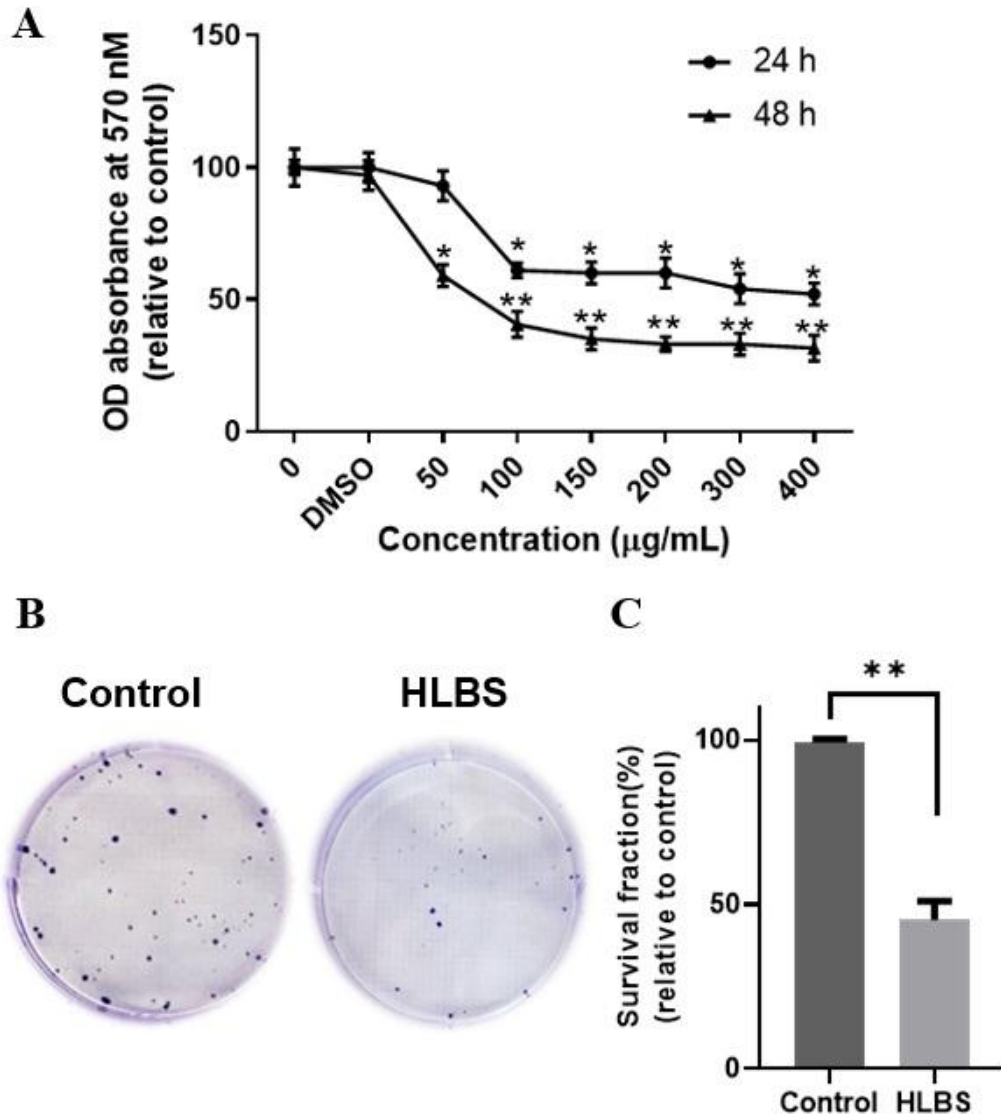


Figure 2. (A) The HLBS cytotoxicity on MNK45 cells at 24 and 48 hours. The inhibitory effect of HLBS was concentration and time-dependent. Data represent mean \pm standard deviation. A comparison between groups was performed using ANOVA test and statistically significant difference ($P < 0.05$) relative to control are denoted by asterisks. (B) Colony formation test at a concentration of 75 $\mu\text{g/ml}$ on MNK45 cell line. (A) HLBS treatment at a concentration of 75 $\mu\text{g/ml}$ resulted in a reduction in colony formation by MNK45 cells compared with the control. (B) After two weeks from the initiation of the test, the survival rate represents as mean \pm standard deviation. Data represent three independent experiments.

DMSO: Dimethyl sulfoxide; OD: Optical density; H: Hours; HLBS: *H. Leucospilota*-derived n-butanol fraction saponins; *: $P > 0.05$; **: $P < 0.01$

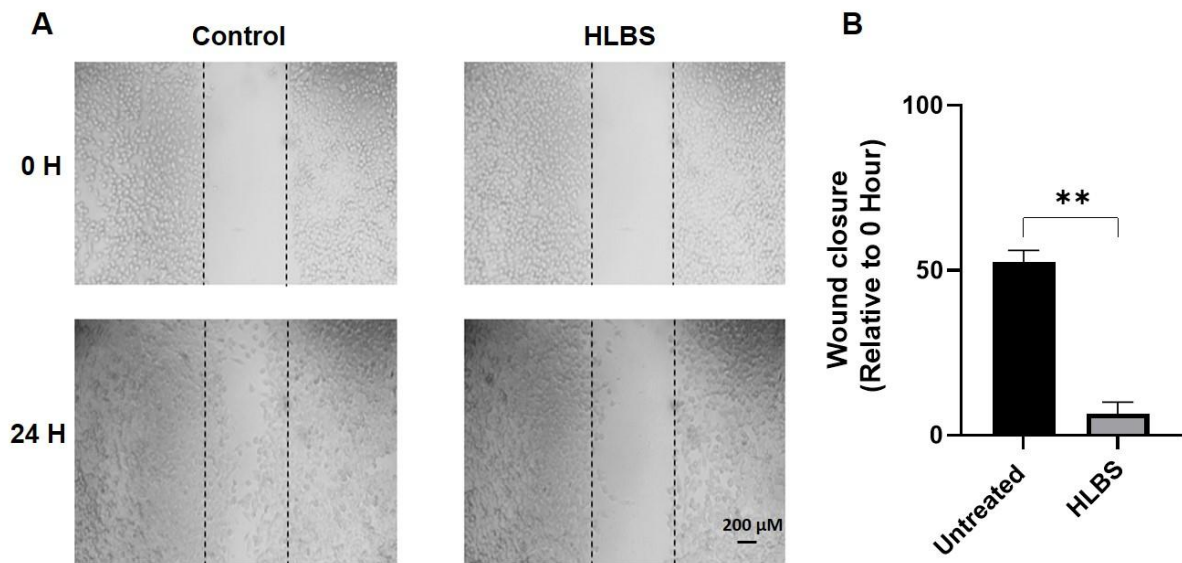


Figure 3. HLBS inhibited the migration ability of MNK45 cells. (A) Microscopic evaluation of Saponin on MNK45 cell line migration. (B) Quantification of wound closure by Image J software represents as mean \pm standard deviation. Data represent three independent experiments.

H: Hours; HLBS: *H. Leucopilota*-derived n-butanol fraction saponins; **: $P < 0.01$

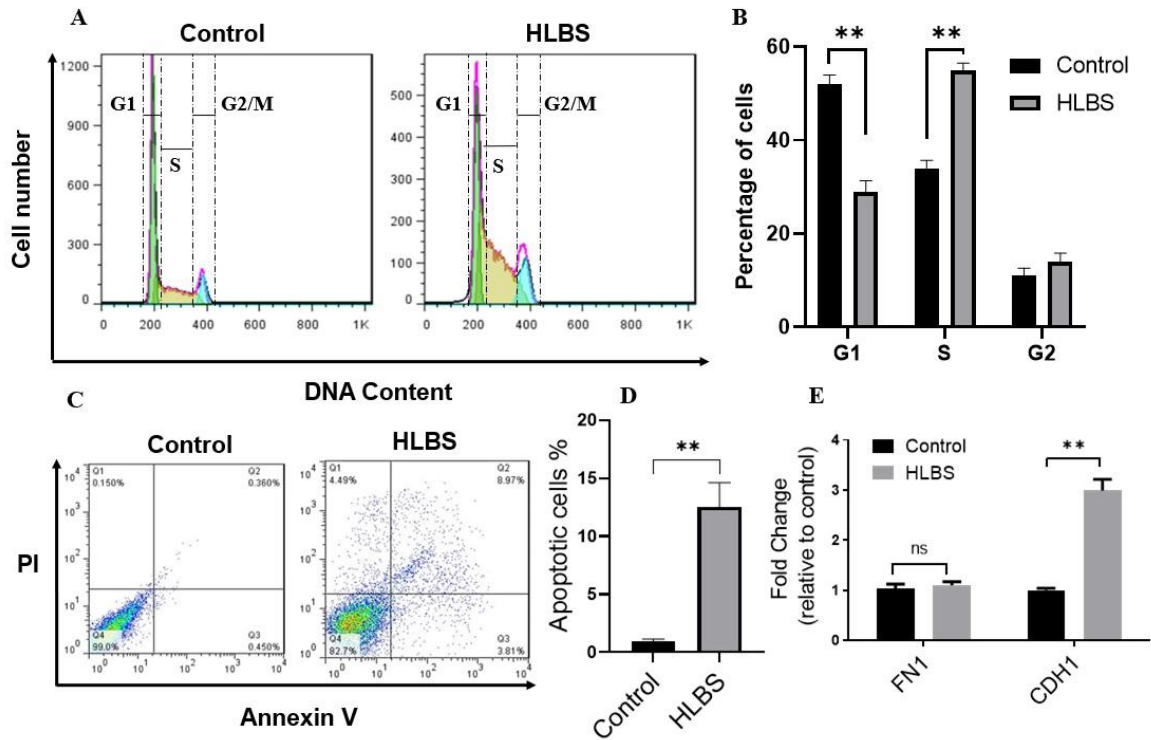


Figure 4. (A) Analysis of cell cycle under treatment of HLBS. (B) The difference in the percentage of cell population in each phase shows that HLBS reduces the G1 phase cell population and increases the S phase cell population. Percentage of cell population represents as mean \pm standard deviation. Data is the representative of three independent experiments. (C) Analysis of apoptosis and necrosis among HLBS-treated cells by flow cytometry at 48 hours after treatment. (D) HLBS at a concentration of 75 $\mu\text{g/ml}$ mainly induced apoptosis in the MNK45 cell line. Percentage of apoptotic cells represents as mean \pm standard deviation. Data is the representative of three independent experiments. (E) Effect of HLBS (75 $\mu\text{g/ml}$) on the expression of CDH1 and FN1 in MNK45 cells. Fold changes represents as mean \pm standard deviation. Data represent three independent experiments and the student t-test was used to compare the two groups.

PI: Propidium iodide; HLBS: *H. Leucospilota*-derived n-butanol fraction saponins; ns: non-significant; G1: Gap1; G2: Gap2; S: synthesis; *: $P < 0.05$; **: $P < 0.01$

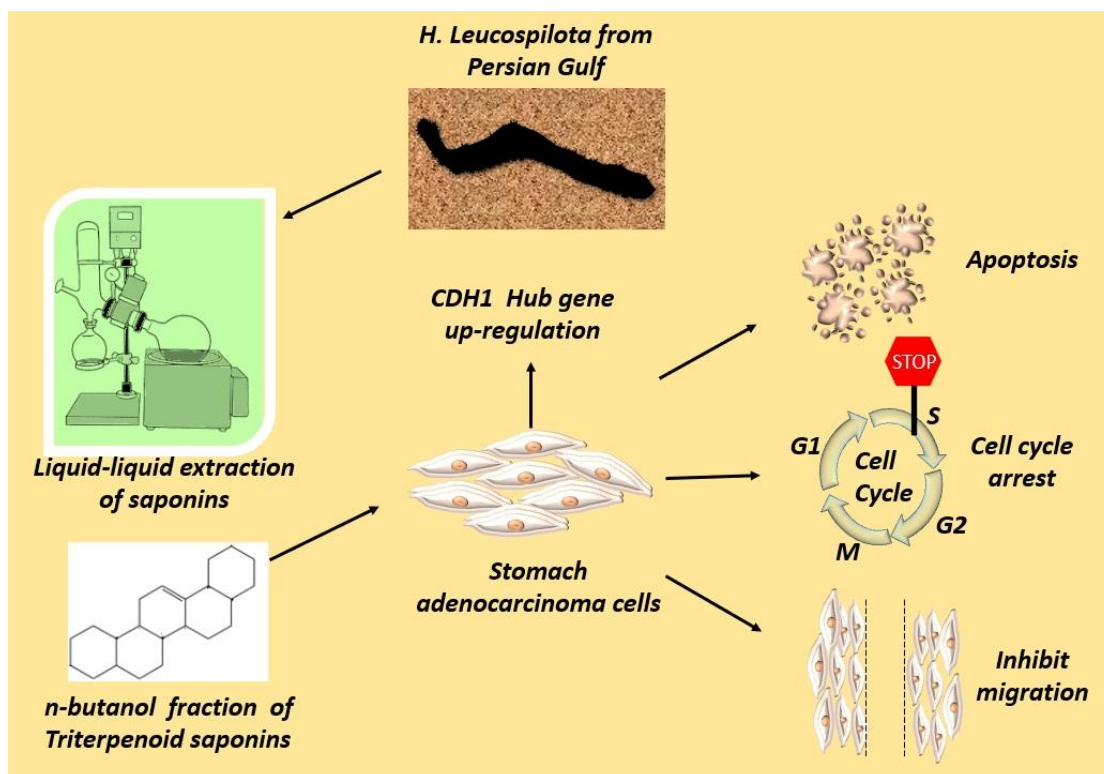


Figure 5. The HLBS extraction and its effects on MNK45 cells. HLBS resulted in a significant decrease in cell viability, and cell migration. Moreover, treatment with 75 $\mu\text{g/ml}$ of HLBS for 48 hours led to an increase of the S-phase and apoptotic cell populations, respectively. HLBS also upregulated the expression of CDH1, as a highly ranked hub gene associated with GC. G1: Gap1; G2: Gap2; M: Mitosis; S: Synthesis